IEEE Access
Multidisciplinary : Rapid Review : Open Access Journal

Received June 7, 2020, accepted June 17, 2020, date of publication July 9, 2020, date of current version July 23, 2020.

Digital Object Identifier 10.1109/ACCESS.2020.3008328

Lubricating Oil Remaining Useful Life Prediction Using Multi-Output Gaussian Process Regression

MONIKA TANWAR AND NAGARAJAN RAGHAVAN, (Member, IEEE)
Engineering Product and Development Pillar, Singapore University of Technology and Design, Singapore 487372

Corresponding author: Nagarajan Raghavan (nagarajan@sutd.edu.sg)

This work was supported in part by the Ministry of Education (MOE), Singapore, through Tier-2, under Grant MOE-2017-T2-1-115, in part by the Temasek SEED under Grant RTDSS1910011, and in part by the National Research Foundation (NRF), Singapore, under Grant NRF2018-SR2001-017.

ABSTRACT Lubricant condition monitoring (LCM) is a preferred condition monitoring (CM) technology for fault diagnosis and prognosis owing to its ability to derive a wide range of information from the system (machine/equipment) state and lubricant state. Given the importance of LCM for maintenance decision support, an accurate and reliable remaining useful life (RUL) prediction framework is necessary. The LCM health information in the form of degradation trends is therefore evaluated using numerous statistical, model-based, and artificial intelligence approaches by various researchers. A multitude of factors widely affects the degradation trends viz. operating conditions, environmental variations, oil replenishments, oil loss, chemical breakdown, etc. These factors increase the complexity of the time-series degradation trends making RUL prediction intractable using several of the standard statistical approaches. Therefore, limited research is available on lubricating oil RUL prediction with these influential factors accounted for. Focusing on the complexity of the degradation trend with oil replenishment effects (ORE), we propose the use of the Gaussian process regression (GPR) model for RUL prediction in this study. The model has an advantage over other data-driven approaches as it is a non-parametric Bayesian method. To exploit prior information and historical data collected, the approach is extended to multi-output GPR (MO-GPR) which effectively defines the correlations between historical degradation trends for similar lubrication systems with the current degradation pattern of a system being monitored in real-time. Three different oil replenishment strategies are considered under MO-GPR to demonstrate the applicability and flexibility of this method.

INDEX TERMS Gaussian process regression, lubrication condition monitoring, prognostics, remaining useful life.

I. INTRODUCTION

To improve system reliability and prolong remaining useful life (RUL), predictive maintenance (PdM) or condition-based maintenance (CBM) strategies rely on efficient condition monitoring (CM). Among numerous online and offline CM technologies [1]–[4], lubricant condition monitoring (LCM) provides early-stage warning ability and multiple other indicators to define the system state [5]–[7]. Wear debris concentration (WDC) is considered as an indicator that can closely define both the lubricant and system state. The recent development of on-line LCM techniques [8]–[10] encourages the use of WDC for system state prediction under PdM / CBM. In practical scenarios, many factors viz. oil replenishment, oil loss, oil filter, and operating conditions affect the WDC and are observable in the form of noise and/or anomalous spikes in the degradation trend. The factors affecting WDC have been considered for wear prediction using the relevance vector machine method by Cao *et al.* [11]. Fan *et al.* [12] discuss the mapping of WDC under different machine wear rates. They use model-based simulations to generate the WDC time-series data and validate these results with experimental data. Several other model-based approaches [13]–[15], statistical approaches [16]–[19] and hybrid approaches [20], [21] have been widely adopted for degradation trend analysis. These approaches pose certain limitations: (1) For model-based approaches, accurate mathematical modeling of the complex system with non-linearity and uncertainty is difficult; (2) Statistical approaches are single feature focused and not able to pick patterns and auto-state

The associate editor coordinating the review of this manuscript and approving it for publication was Zhaojun Li.

observations, and tend to be harder for modeling of non-monotonic degradation trends; (3) For hybrid methods, modeling of the complex system considering the environmental and external factors still remains a challenge.

Observing the limitations of standard approaches, we consider an artificial intelligence (AI) approach here with the ability of pattern recognition, prediction, and stochastic estimation. The AI approach utilized should recognize the degradation pattern and map the relationship between the response and input data using a supervised machine learning (ML) technique.

For example, logistic regression as a predictive analysis tool is used by various researchers due to its ability to handle nonlinear effects. Literature shows the applicability of logistic regression for decision making on feature contribution to prediction, estimation of maintenance inspection intervals and oil diagnostics, etc., [22]–[28]. However, the use of logistic regression is limited by constraints viz. overfitting, inappropriate to continuous outcomes, and requirement of large datasets. The Random Forest (RF) method is another supervised machine learning technique for LCM that uses individual decision tree outputs to estimate the parameters [29]. RF resolves the overfitting issue of the decision tree approach by averaging the results, also catering to missing data which may be highly prevalent in large data sets. The use of the RF approach is however limited due to modeling complexity and computational load. Du *et al.* [30] effectively use Vector autoregression and Kalman filter for time series modeling of wear debris concentration data. The residual data obtained from Kalman filter, then work as an input to the Hidden Markov Model for state prediction. The Kalman filter is useful in feature reduction and approximation scenarios with multiple inputs and is used as a recursive methodology to obtain the conditional failure distribution [31] and state estimation [32]. The non-linear growth in degradation will affect the performance of a linear model, i.e. Kalman filter requiring many assumptions. Wu *et al.* [33] use a support vector data description method for wear stage characterization considering wear mechanisms that remain the same within a stage i.e. wear is a gradual mechanism unlike brake failure and its performance remains the same within a stage. There is insufficient literature in LCM that deals with using Autoregressive moving average (ARMA), Vector autoregression moving average (VARMA), Gaussian process regression (GPR), and Bayesian dynamic linear models (BDLM) for prognosis. The authors of this study have attempted autoregressive integrated moving average (ARIMA) and BDLM [35] in their previous work and discovered that the model should be able to predict both linearity and non-linearity of degradation signals with discontinuities.

To predict LCM data, a Bayesian method with probabilistic bounds for uncertainty may provide better efficacy. The Gaussian Process regression (GPR), as a non-parametric Bayesian method, offers the advantage of modeling complex systems with several parameters. GPR has been successfully applied to a wide range of prognostic applications viz. battery degradation [36], light-emitting diode degradation [37], bearing degradation [38], and financial predictions in the stock market [39] etc.

In the case of LCM, the literature lacks GPR based degradation predictions. Moreover, existing LCM analysis techniques lack predictive ability when the data is polluted by external factors listed out earlier. This work is a novel attempt in the field of tribology that considers the use of multi-output GPR (MO-GPR) to model the lubrication degradation and to predict the RUL. Wear debris concentration is selected as the degradation index representing the state of the lubricating oil.

The study moving forward is structured as follows. Section II describes the WDC data generation using model-based simulation and data denoising strategy to improve the prediction accuracy. The fundamentals of single output (SO) and multi-output (MO) GPR are then discussed in Section III. Section IV presents the prognosis results for five data sets using MO-GPR and discusses the accuracy of the model predictions for RUL. Finally, Section V concludes the work highlighting the relevance of GPR for LCM, also proposing further ideas to be explored in this domain.

II. DEGRADATION DATA – MODELING AND SIMULATION

Wear occurs at contact surfaces of tribological components in a mechanical system. Lubricating oil is used to reduce wear and friction between contact surfaces. In this study, a simple lubrication system is considered with four components → oil tank, oil filter, oil pump, and tribo-component. Wear debris generated in the system is simulated using a model-based simulation framework proposed by Fan *et al.* [12]. WDC is mapped for increasing wear rate. The assumptions considered for the simulation are as follows:

(1) Homogenous and instantaneous mixing of wear debris with replenished oil.
(2) Oil replenishments follow three strategies → (a) oil replenishments at fixed time events, (b) oil replenishments at different time events and (c) oil replenishment at times when WDC crosses a preset threshold.
(3) The system is already in the wear-out phase of the bathtub curve.

The WDC is related to the wear rate function and exponential attenuation function as given by Ref. [12]:

$$C(t) = \frac{m(t) * r(t)}{V_0 + V_r * t - V_q * t} \tag{1}$$

$$r(t) = \exp(-kt) \times 100\% \tag{2}$$

$$k = \left[\left({}^{1}\!/_{\beta_x}\right) Q + \Psi\right] \Big/ V_0 \tag{3}$$

where $C(t)$ is the wear debris concentration (ppm), $m(t)$ is the wear rate (mg/min), $r(t)$ is attenuation function for wear debris removal in the lubrication system, k is the attenuation coefficient, β_x is the beta ratio for oil filtration, V_0 is the initial volume of lube oil in the tank, V_r is the fresh oil replenishment rate, V_q is the oil loss rate, Q is the nominal oil flow through the filter (L/min) and Ψ is the debris loss factor due to other factors (sedimentation, comminution, etc.).

One such WDC trajectory generated from the model-based simulation with the oil replenishment effect (ORE) is shown in Fig. 1. The ORE comprises of three components as will be explained below.

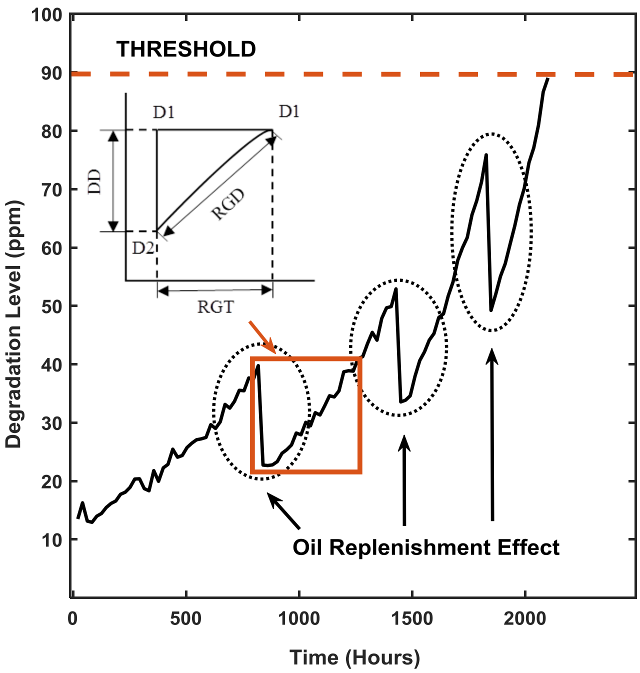

FIGURE 1. Lubrication oil degradation trajectory with oil replenishment effects (ORE).

The failure threshold is set to 90 ppm WDC for test data. The simulated degradation data represents the dependency of WDC on the wear rate as described by Eqn. (1). This work focuses on determining the learning ability of MO-GPR from correlations of multiple historical patterns with discontinuities. Following the identical trends of WDC and wear rate for all degradation patterns, the historical data is then time terminated with reference to the test data threshold.

1. Degradation Drop (DD): The drop-in degradation level is caused by factors viz. oil filter, oil replenishment, tribo- component replacement, and operating environment. This work considers DD to be solely due to oil replenishment and assumes the replenishment to be instantaneous, which is a reasonably good assumption considering the relatively much longer time spans of system operation.
2. Replenishment Generated Degradation (RGD): After DD, replenished oil mixed with remaining oil starts degrading and takes time to reach the degradation level D_1 i.e. degradation level before oil replenishment. This phase of degradation is nomenclated as replenishment generated degradation (RGD). The parameters D_1 and D_2 represent the degradation levels before and after oil replenishment. In our case here, it depicts the WDC just before and after oil replenishment.
3. Replenishment Generated Time (RGT): RGT is the oil life extension due to delayed degradation after ORE.

Data sets are simulated for three oil replenishment strategies as discussed below (Table 1 summarizes the data terminology):

Data I: Under this category, the data is simulated for Strategy I i.e., oil is replenished at fixed time points. DD is assumed to follow an exponential distribution based on observation from the literature that oil replenishment quantity increases with operating time [40]. Fig. 2 shows the simulated WDC trends with periodic oil replenishments termed as periodic degradation trends (PDT).

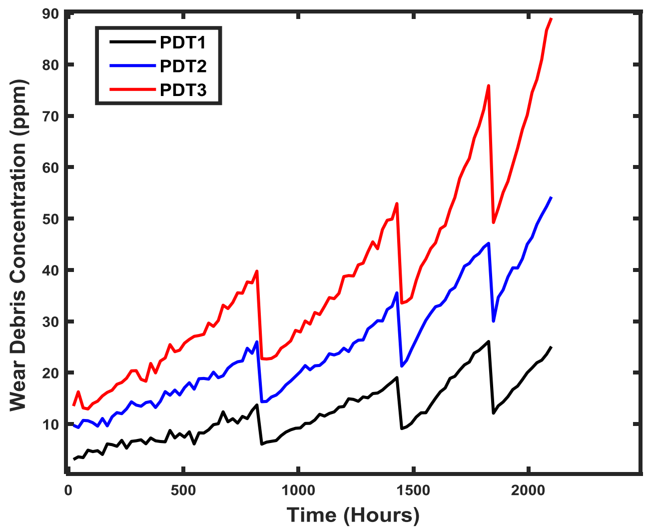

FIGURE 2. Simulated periodic degradation trends (PDT) corresponding to Data I.

Data II: Here, the data is simulated for Strategy II i.e., oil is replenished at random time intervals. Fig. 3 shows the WDC trends for Data II termed as aperiodic degradation trends (APDT).

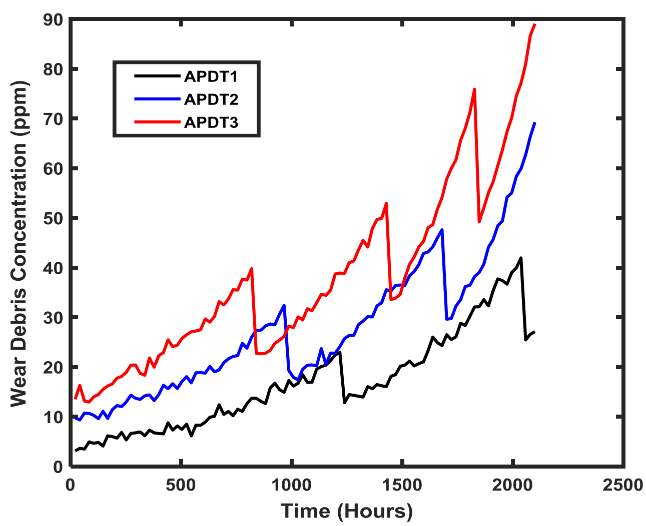

FIGURE 3. Simulated aperiodic degradation trends (APDT) corresponding to Data II.

Data III: We consider data generation for Strategy III, which follows a threshold-based oil replenishment. Oil is replenished as the WDC crosses the set upper threshold. The DD is fixed for all oil replenishments. The data is time terminated for similar time lengths as Data I and Data II. Fig. 4 shows the WDC trends termed as degradation trends (DT). WDC will be referred to as degradation level in the remaining text.

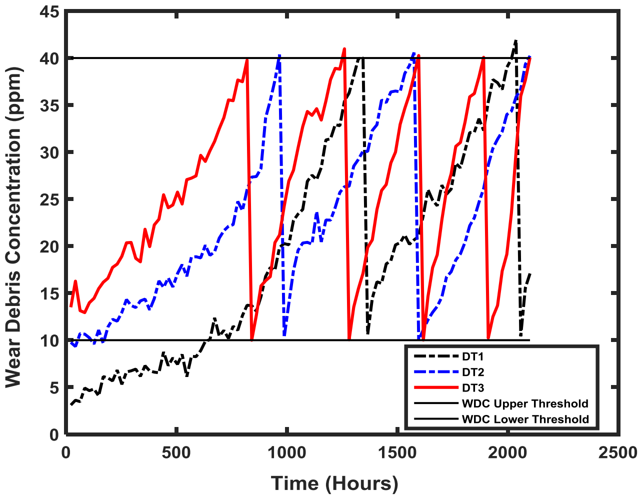

FIGURE 4. Simulated threshold based degradation trends (DT) corresponding to Data III.

Data Denoising (Correction) - To improve prediction efficiency, the data is de-noised for DD. The authors in their previous work in Ref. [34] discuss the lubricating oil top-up effect on degradation prediction and suggest the degradation data collection before oil top-up to improve prediction accuracy. Therefore, in the present work, the oil top-up effect i.e. DD, is filtered from the data. Data I, II, and III are generated using model-based simulation as discussed earlier. It comprises of natural degradation, DD, RGD, and RGT with m number of observation points and can be defined as:

$$D(t) = \{D_i(t), i = 1, 2 \ldots m\} \tag{4}$$

Data II and III are corrected for n number of DD. The corrected data, D_C is expressed as:

$$D_c(t) = D_i(t) + \sum\nolimits_{j=0}^{n} DD_j \tag{5}$$

where DD_j, (j = 0, 1 . . . , n) denotes the degradation drop in Eqn. (5) with a cumulative summation of the DDs in degradation values (WDC). If the discontinuities are filtered from the degradation signal, we arrive at the base pattern of the degradation trend.

Authors have observed from their previous work in Ref. [35] that a nonlinear degradation pattern is a mix of linear (i.e. base degradation) and nonlinear components (i.e. impact of external events). The prediction model, therefore, needs to be tested with both linear and nonlinear components of degradation patterns for its aptness. To refine the degradation signal more, the complete ORE needs to be filtered from the signal [36].

TABLE 1. Data terminologies used in this study.

Data Sets	Nomenclature
Data I	Periodic Degradation Trends (PDT): PDT 1, PDT 2, PDT 3
Data II	Aperiodic Degradation Trends (APDT): APDT 1, APDT 2, APDT 3
Data III	Degradation Trends (DT): DT 1, DT 2, DT 3
Data IV	Corrected Aperiodic Degradation Trends (CAPDT): CAPDT 1, CAPDT2, CAPDT3
Data V	Corrected Degradation Trends (CDT): CDT 1, CDT 2, CDT 3

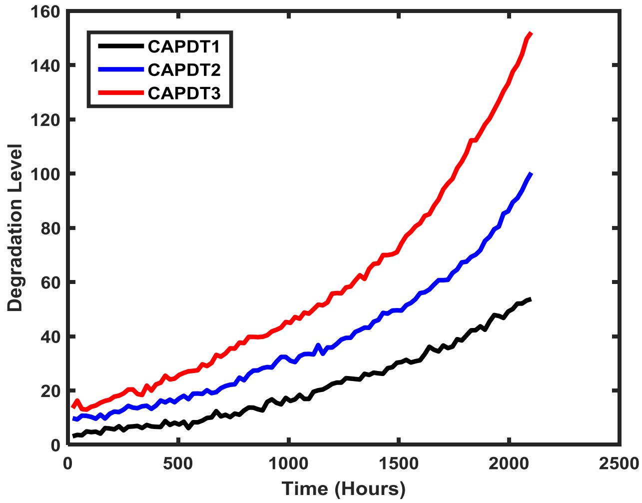

FIGURE 5. Corrected aperiodic degradation trends (CAPDT) for Data II, i.e. Data IV.

A prediction model suitable for analyzing the base signal (linearity) and the signal with discontinuities (non-linearity) should be considered for further analysis. Fig. 5 depicts the de-noised trend for Data II and is termed as Data IV or corrected aperiodic degradation trend (CAPDT). The correction for Data I is not required as it will follow the same patterns as Data IV (this is because the magnitude of jumps for the simulated Data Sets I and II are the same; the only difference is in the timing of the jumps). Similarly, de-noising is carried out for Data III and termed as Data V or corrected degradation trend (CDT) and is shown in Fig. 11.

III. GAUSSIAN PROCESS REGRESSION (GPR)

A. SINGLE OUTPUT GAUSSIAN PROCESS REGRESSION (SO-GPR)

GPR is a Bayesian regression technique whose joint distribution is a multivariate normal distribution for a finite subset of outputs. It is parameterized by the mean function and covariance function. For scalar inputs and outputs, the Gaussian Process is defined as:

$$f(t) \sim N(\mu(t), k(t, t')) \tag{6}$$

where t is the time, $\mu(t)$ is the mean function and $k(t, t')$ is the covariance function. For regression purpose, the prior mean

$\mu(t) = E[f(t)]$ is assumed to be zero. The covariance is specified by the chosen kernel and there are many options to choose for the kernel function including constant, linear, Matern, radial basis function and composition of multiple kernels. The popular squared exponential function is used to represent the covariance here. It is a stationary kernel and is defined by:

$$k_{SE}(t, t') = \sigma^2 exp\left(-\frac{(t-t')^2}{2l^2}\right) \tag{7}$$

where the hyper-parameter variance is denoted by σ, the length scale is denoted by l with a controlled scaling of functions, $f(t)$ and t. Using the labeled n training points of degradation data $y(t_i)$ with joint prior distribution, $T = \{(t_i, y_i)\}_{i=1}^{n}$, and with a test point t^*, prediction can be made using the conditional distribution:

$$p((y^* \mid t^*, t, y) = \mathcal{N}\left(y^* \mid m^*, \sum^{*}\right) \tag{8}$$

where

$$m^* = K\left(t, t^*\right)^T K(t, t^*)^{-1} y \tag{9}$$

$$\sum^{*} = K\left(t, t^*\right) - K\left(t, t^*\right)^T K\left(t, t^*\right)^{-1} K\left(t, t^*\right) \tag{10}$$

Hyperparameters σ, l and noise variance θ are estimated by minimizing the negative log-likelihood (NLML):

$$\{\sigma, l, \theta\} = arg \min_{\sigma,l,\theta} NLML \tag{11}$$

$$where \quad NLML = -logp\,(y \mid t, \theta) \tag{12}$$

B. MULTI-OUTPUT GAUSSIAN PROCESS REGRESSION (MO-GPR)

The MO-GPR considers a pair of variable labels and time as input to provide variable value as output. The Gaussian nature of conditional and marginal probabilities under MO-GPR provides analytical posterior distribution conditioned on degradation observations. The prediction uncertainty can then be estimated using mean and variance of the predictive distribution. MO-GPR considers correlations between similar patterns of degradation and a new covariance function is formed for a single time series with additional input g based on different observed historical time-series patterns:

$$k_{MO-GPR} = k_g(g, g', \theta_g) \times k_t(t, t', \theta_t) \tag{13}$$

where k_g depicts the correlation between different degradation patterns (time series data) and k_t defines the covariance with respect to degradation cycles for the current system unit being monitored. The covariance matrix can be expressed as:

$$K_{MO-GPR}(T, d, \theta_g, \theta_t) = K_g\left(g, \theta_g\right) \otimes K_t\left(t, \theta_t\right) \tag{14}$$

Where d refers to a single degradation time series, $\otimes$ is the Kronecker product and $\{\theta_g, \theta_t\}$ are the hyper-parameters which can be obtained by maximizing the log-likelihood. After defining the covariates, the parameterization of the correlation can be achieved using free form parameterization approach [41] with the following covariance matrix, K_c, for $\mathcal{D}$ degradation patterns:

$$K_c = \begin{bmatrix} \theta_{c,1} & 0 & 0 \\ \theta_{c,2} & \theta_{c,3} & 0 \\ \vdots & \ddots & 0 \\ \theta_{c,k-\mathcal{D}+1} & \theta_{c,k-\mathcal{D}+2} \;\; .. & \theta_{c,k} \end{bmatrix} \tag{15}$$

The parameterization uses Cholesky decomposition designed for a positive definite matrix. The diagonal elements of this matrix represent the correlation of degradation of the same unit and the non-diagonal elements denote correlation in degradation between different units (data sets). Therefore, a sum total of k hyper-parameters with $k = \mathcal{D}(\mathcal{D}+1)/2$ fully describes the degradation trend correlations. The predictive distribution is then defined using Eqn. (8). The MO-GPR is applied to all five "processed" sets of WDC data comprising 400 historical data points. The results are presented in the next section in detail.

IV. RESULTS AND DISCUSSION

In this section, the GPR based RUL prediction results for all data sets are presented and discussed. Table 2 summarizes the prediction errors, expressed in terms of the root mean square errors (RMSE) written as:

$$RMSE = \sqrt{\sum_{i=1}^{n} \frac{(v_i - z_i)^2}{n}} \tag{16}$$

where v_i is the predicted degradation value, z_i is the observed degradation value and n is the number of observations. Table 2 lists the RMSE values at different percentages of training data sets i.e. 20%, 40%, 60%, and 80% using SO-GPR and MO-GPR methodology for all degradation data defined in Section II. The training data sets are the actual data introduced to the model before testing the model for pattern recognition, mapping and replication.

TABLE 2. RMSE values for SO-GPR and MO-GPR predictions.

Data	20% Training	40% Training	60% Training	80% Training
Data I	2.516	2.628	2.050	1.962
Data II	7.480	6.941	6.319	5.688
Data III	8.791	8.586	7.826	4.645
Data IV	2.402	1.952	1.962	1.937
Data V	4.275	5.252	4.415	4.033
Data I (SO-GPR)	5.482	4.964	3.673	2.814
Data II (SO-GPR)	8.485	8.173	7.491	6.372
Data III (SO-GPR)	10.19	9.528	8.725	7.168

As a comparison, Table 3 presents the RMSE values for test data prediction at 20%, 40%, 60%, and 80% training levels using Autoregressive Integrated Moving Average (ARIMA) and Bayesian Dynamic Linear Model (BDLM) methods as presented by Tanwar and Raghavan in Ref. [35]. Note that the

TABLE 3. RMSE values for ARIMA and BDLM predictions [35].

MODEL	20%	40%	60%	80%
ARIMA I	63.45	92.7	14.257	13.292
ARIMA II	17.991	15.423	24.108	9.758
ARIMA III	4.09 (35%)	4.4792	13.721	11.495
ARIMA IV	-	3.10/2.41/ 1.025/ -	1.61/3.57/ 5.10 /1.09	1.10/1.53/ 1.77/2.79
BDLM I	22.65	9.32	14.19	17.650
BDLM II	27.57	34.64	39.376	41.577
BDLM III	13.537	12.251	15.886	19.770
BDLM IV	-	6.13/17.16/ 35.27/48.08	1.53/5.36/ 11.51/26.71	1.32/1.94 / 4.97/13.5
BDLM V	18.396	15.438	26.464	20.311

test data prediction at 60% training data under ARIMA IV depicts the RMSE values for degradation prediction during four top-up intervals i.e. 1.61 / 3.57 / 5.10 / 1.09. In other words, 1.61 is the RMSE value for the first top-up interval with 60% training data set, 3.57 is RMSE value for the second top-up interval with 60% training data and similarly the RMSE values for the remaining two top-up intervals are 5.10 and 1.09.

In the context of the study here, it is important to mention that the definition we provide to SO-GPR is different from the standard interpretation. In general, SO-GPR involves training only using the current data set (no prior historical time series data set) for any future predictions. However, given that the WDC values exhibit singularities (negative jumps) during every maintenance (oil replenishment) event, prediction of the future trends without any historical time series data set would certainly yield very poor results as the abrupt changes in the WDC pattern would not be captured. Therefore, in the study here, we have regarded SO-GPR to be the case when there is exactly one full historical time series data available from a similar unit inclusive of the impact of oil replenishment in addition to the current data being monitored for the unit under study.

A. GPR ANALYSIS OF DATA I

In this subsection, the WDC data is generated using model-based simulation [12]. The degradation level is defined by WDC (in units of ppm) at different operating times and periodic oil replenishments are considered with variable oil replenishment effects (ORE).

The SO-GPR method is first applied to three degradation data sets (Data I, Data II, Data III). The single output GPR poses a limitation for degradation patterns with negative or positive jumps [31], which makes it inept for the present work. The prediction results using SO- GPR for Data I, II, and III are shown in Figs. 6 (a, b, c).

The RMSE values for the prediction at 20% trained data are 5.45, 8.48, and 10.19 for Data I, II, and III respectively, which is significantly higher than that for the MO-GPR, as we will discuss further. The MO-GPR method is applied to Data I considering two degradation trends (PDT1, PDT2)

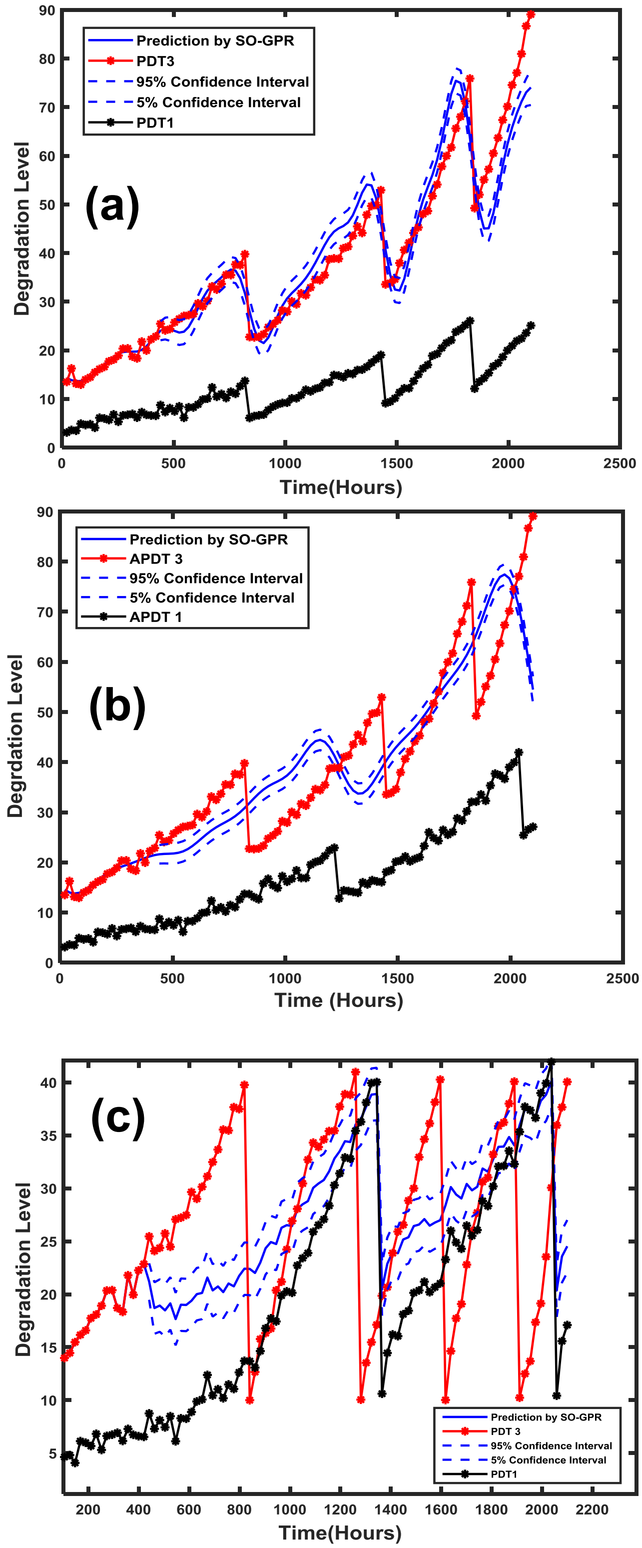

FIGURE 6. Prediction by SO-GPR for (a) Data I, (b) Data II, and (c) Data III at 420 hours. The SO-GPR prediction is suitable for degradation trend tracing for the case of periodic oil replenishment as shown in Fig (a), whereas SO-GPR analysis in Figs. (b) and (c) shows its inability to capture the aperiodicity in degradation trend for irregular patterns of replenishment. Availability of multiple degradation trend traces under MO-GPR will help improve the prediction accuracy for such irregular scenarios.

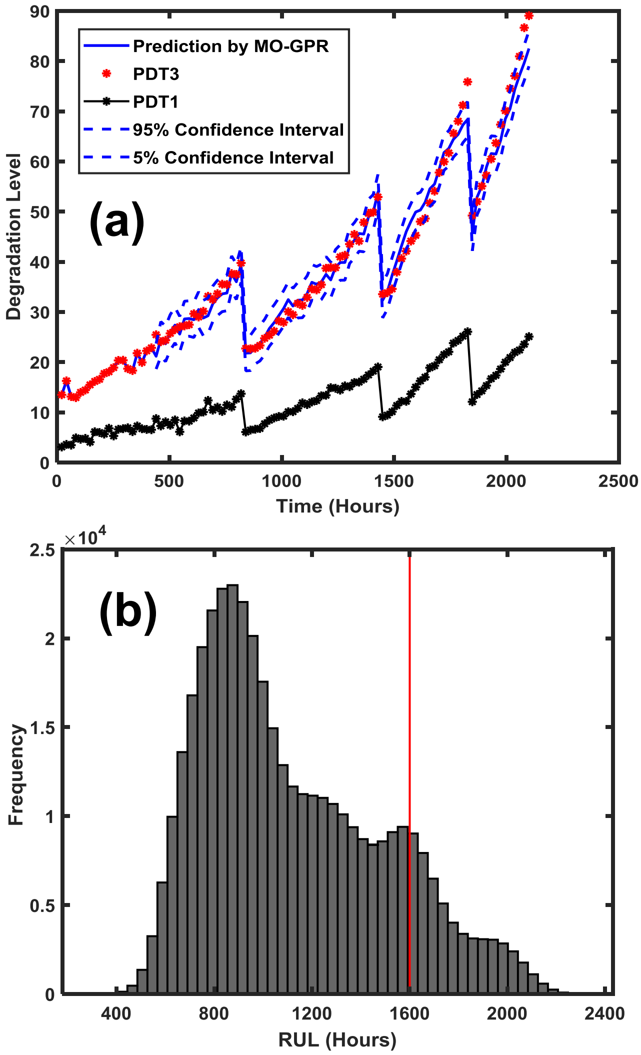

FIGURE 7. (a) Prediction by MO-GPR for Data I (Periodic degradation trend (PDT)) at 420 hours and (b) the corresponding RUL histogram with the red line representing the "true RUL". Note that all the time-series training data sets are not shown in (a) for better visibility of the results.

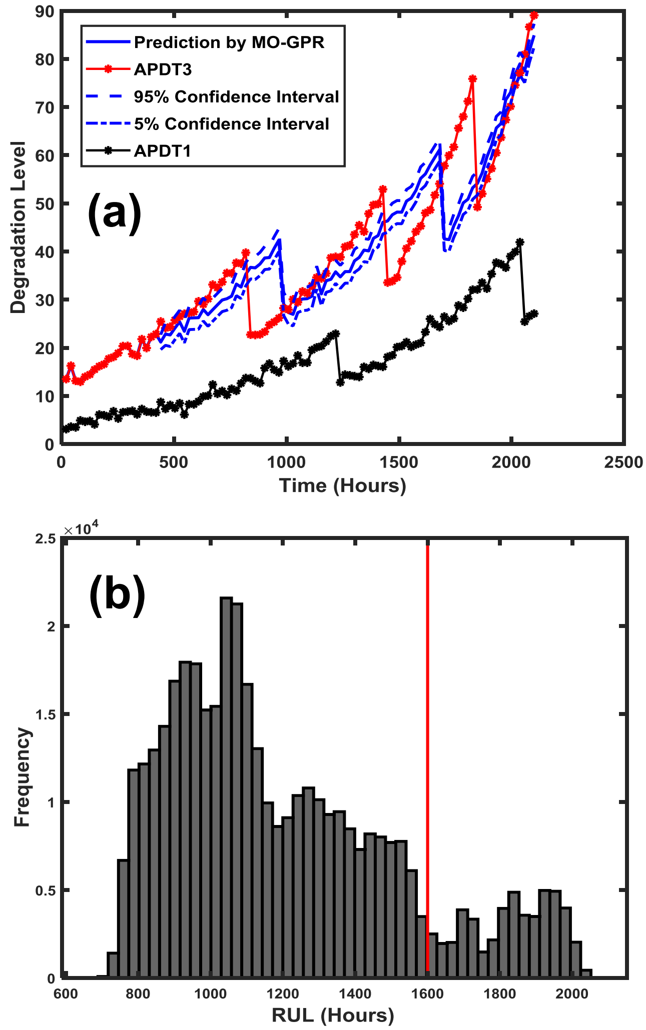

FIGURE 8. (a) Prediction by MO-GPR for Data III (Threshold based degradation trend (DT)) at 900 hours and (b) the corresponding RUL histogram with the red line representing the "true RUL". Note that all the time-series training data sets are not shown in (a) for better visibility of the results.

for algorithm training and uses 20%, 40%, 60%, and 80% of the third degradation trend (PDT3) to make the prediction. Fig. 7(a) shows the predicted lubricant degradation trend and Fig. 7(b) plots the respective remaining useful life (RUL) histogram. The red vertical line in Fig. 7(b) denotes the true RUL.

The root mean square errors (RMSE) are estimated for the predicted trend. As is evident from the RMSE values i.e. 2.51, 2.62, 2.05, 1.96, for 20%, 40%, 60% and 80% trained data, the prediction accuracy of MO-GPR is considerably high even for a small data set. This shows that MO-GPR has a good learning ability from historical patterns with negative jumps. In addition, it is worth noting the SO-GPR's inability to trace the degradation trend with aperiodic oil replenishments in Figs. 6(b) and 6(c). Therefore, moving forward, we will only continue to explore the use of MO-GPR for the other data sets → Data II, Data III, Data IV and Data V.

B. GPR ANALYSIS OF DATA II

Here, the WDC data is generated using the simulation method as described in Section II assuming aperiodic oil replenishments with varying ORE. The MO-GPR predicts the degradation trend (APDT-3) using previously learnt degradation trends of APDT-1 and APDT-2 used for training.

The prediction result is shown in Fig. 8 with the corresponding RUL histogram. The RMSE values for predicted degradation trends are 7.48, 6.94, 6.31 and 5.68 for 20%, 40%, 60% and 80% of training data, respectively. The estimated prediction errors are relatively higher here as compared to Data I due to the aperiodic oil replenishments in comparison to the regular (periodic) replenishments earlier.

C. GPR ANALYSIS OF DATA III

In this subsection, the WDC is simulated for an operating region between the lower and upper WDC thresholds assuming aperiodic oil replenishments. The case of periodic oil replenishment is not feasible since the two strategies cannot coexist i.e. threshold-based replenishment and periodic replacement at the same time. The upper threshold defines the maximum permissible level of WDC in the lubricating oil and the lower threshold defines the minimum permissible WDC level that needs to be maintained after oil replenishment so that a well-defined system operating range can be adhered to.

The predicted trend with the RUL histogram is shown in Fig. 9. The RMSE for predicted values are 8.79, 8.58, 7.82, and 4.64 corresponding to 20%, 40%, 60% and 80% training data, respectively. The errors are more than that reported for Data I and Data II. This indicates that the model's predictive ability decreases for aperiodic oil replenishment strategy and threshold-based strategy. To overcome the model's limitation, the authors here suggest denoising of the data as described in Section II.A. The prediction results after data denoising are presented in the next sub-section.

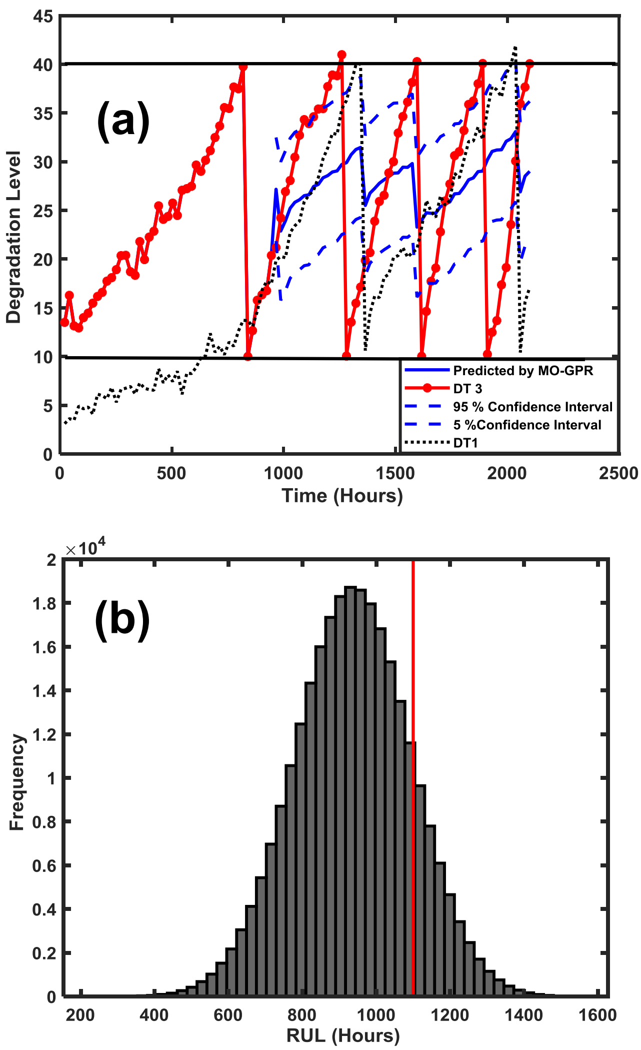

FIGURE 9. (a) Prediction by MO-GPR for Data II (aperiodic degradation trend (APDT)) at 420 hours and (b) the corresponding RUL histogram with the red line representing the "true RUL". Note that all the time-series training data sets are not shown in (a) for better visibility of the results.

D. GPR ANALYSIS OF DATA IV

Data IV refers to the corrected aperiodic degradation trend (CAPDT) used for training and prediction. The prediction for corrected data sets is carried out again using MO-GPR. The prediction results with the RUL histogram for Data IV are shown in Figs. 10 (a, b). The prediction errors are 2.402, 1.952, 1.962 and 1.937 for 20%, 40%, 60%, and 80% training data respectively, clearly showing a marked reduction in error for corrected data in comparison to the noisy (spiky) data i.e. Data II.

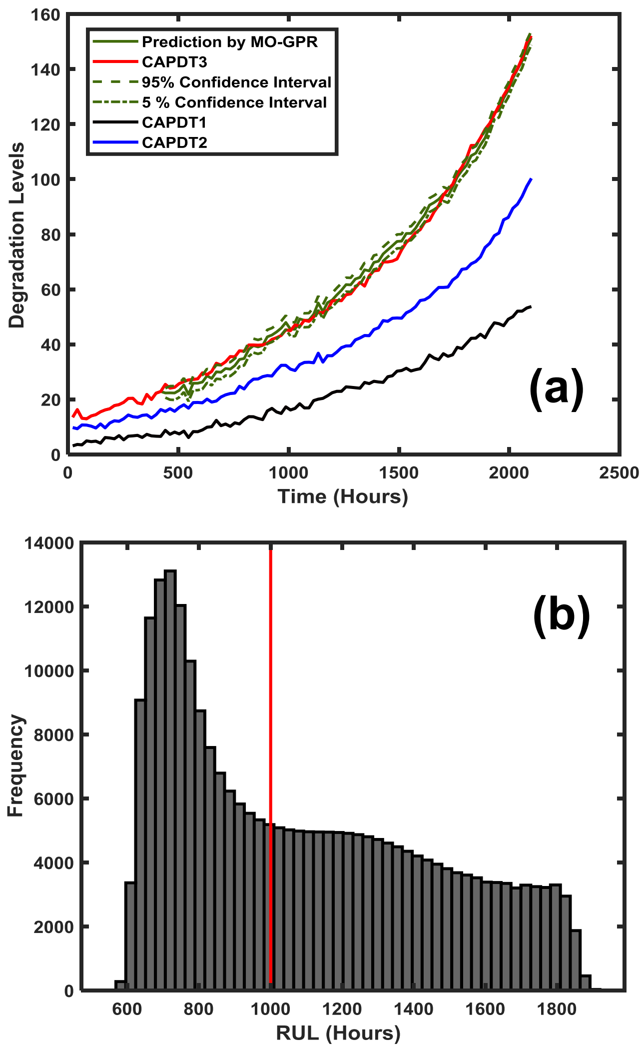

FIGURE 10. (a) Prediction by MO-GPR for Data IV (CAPDT) at 420 hours and (b) the corresponding RUL histogram.

E. GPR ANALYSIS OF DATA V

Data V corresponds to the corrected degradation trend (CDT) for Data III, used for training and prediction. The prediction results with RUL histogram for Data V are shown in Fig. 11 (a, b). The prediction errors for the denoised data are again

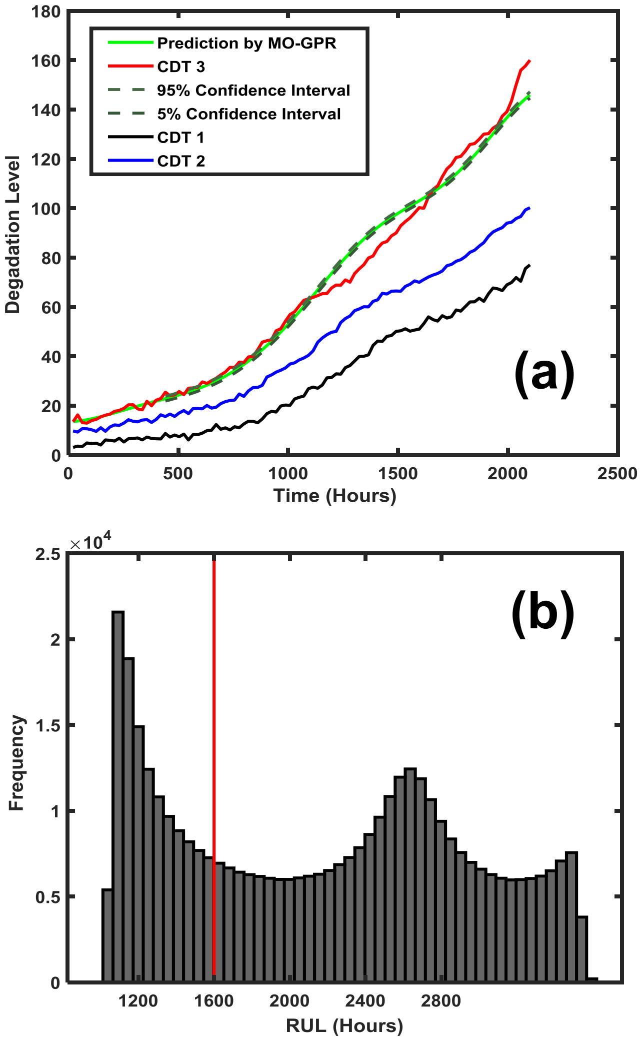

FIGURE 11. Prediction by MO-GPR for Data V (CDT) at 420 hours and the corresponding RUL histogram.

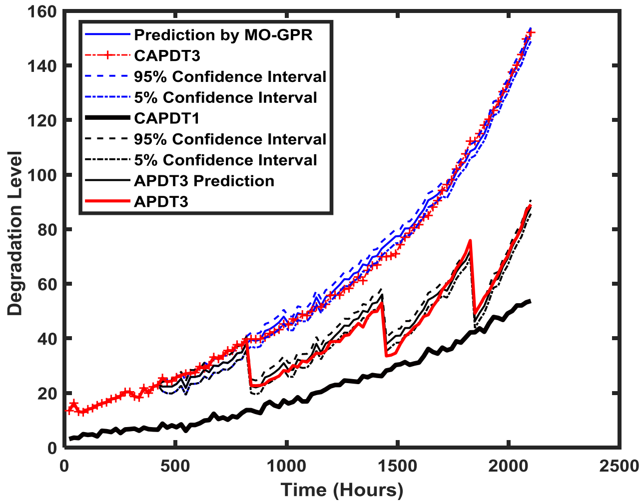

FIGURE 12. Prediction by MO-GPR for Data II and IV at 420 hours. Note that all the time-series training data sets are not shown here for better visibility of the results.

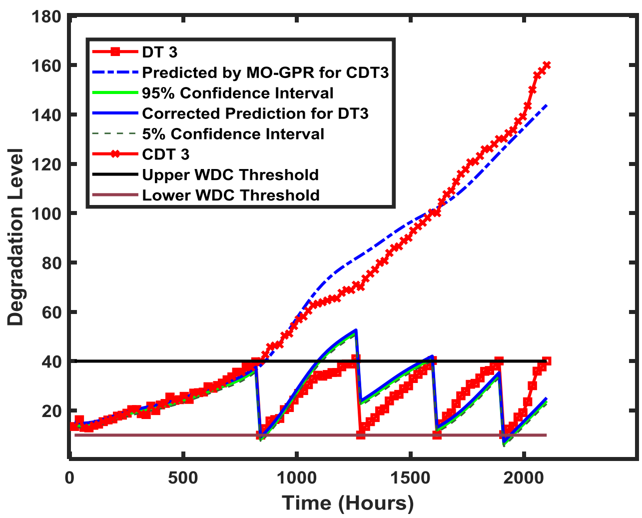

FIGURE 13. Prediction by MO-GPR for Data III and V at 420 hours. Note that all the time-series training data sets are not shown here for better visibility of the results.

lower at 4.275, 5.252, 4.415, and 4.033 for 20%, 40%, 60%, and 80% training data when compared to the raw data set (Data III).

The prediction values for Data IV and Data V are further modified for DD to visualize the prediction accuracy with Data II and Data III. The modified predicted degradation traces can be formulated as:

$$PD\,(t) = PD_i\,(t) - \sum\nolimits_{j=0}^{n} DD_j \tag{17}$$

Where PD is the predicted degradation value. The modified prediction results using Eqn. (17) are shown in Figs. 12 and 13. DDs are negative jumps in the degradation trends induced by oil replenishments (external event). The removal of DDs from degradation signal provides base degradation pattern, i.e. WDC generated from wear mechanism only. The DD removal from degradation trend increases prediction accuracy, using MO-GPR. The discontinuities are then introduced in the predicted signal to visualize the conformity of predicted trends with raw degradation trends i.e. Data II and Data III.

With the comprehensive analysis presented here on RUL prediction using different simulated LCM data sets and their processed versions, the following inferences may be drawn from the MO-GPR study here:

1. The MO-GPR shows efficacy and accuracy in modeling complex degradation trends of LCM, which other traditional prediction methods generally cannot.
2. Prediction errors increase with aperiodic and threshold-based oil replenishments.
3. The prediction based on a single historical pattern for algorithm training (SO-GPR) shows a much higher error than two historical data sets (MO-GPR). Table 2 shows the RMSE values for all data sets with the comparative reduction in errors.

4. Table 3 provides RMSE values for predictions using ARIMA and BDLM methods [35]. A comparative examination of RMSE values suggests MO-GPR as a more suitable approach for lubrication degradation prediction under frequent oil replenishments. In comparison to the deterministic predictions from ARIMA and BDLM, MO-GPR also provides the distribution of the RUL, which is a big advantage for risk-informed predictive maintenance planning.
5. Prediction errors for Data I (periodic degradation trends) without considering ORE are approximately alike to Data I. It shows the model's suitability to accurately predict all patterns (even if they have singularities or kinks or abrupt changes/spikes in values) of periodic replenishment-based degradation trends.
6. In the case of aperiodic degradation trends (Data II and Data III), data de-noising is first necessary in order to obtain acceptable prediction results.
7. MO-GPR accounts for both the linear (base degradation pattern due to wear mechanism) and non-linear (negative jumps due to oil top-up) components of the raw degradation signal. Larger historical datasets will be needed to improve the prediction accuracy for irregular oil top-up scenario i.e. Data II.

V. CONCLUSION

This study presented a robust and generic lubricating oil wear debris degradation forecasting approach using multi-output Gaussian process regression (MO-GPR). In lubrication condition monitoring, wear debris concentration (WDC) is a good representative of the oil state and forms a non-stationary time series data. The applicability of MO-GPR for non-stationary WDC data with discontinuities arising from regular and irregular oil replenishment effects is well demonstrated and exemplified in this study. In contrast to the MO-GPR framework here, traditional statistical approaches presented in other studies lack the predictive ability for such complex realistic patterns of data with anomalous spikes (negative jumps in WDC value) that represent the purposeful interventions in the system. The MO-GPR appears to be highly effective in learning from small and sparse learning data sets and provides good prediction results even for very complex patterns of time series data. We tested the applicability of MO-GPR here using three different simulated data sets of oil debris wear. The computational time using MO-GPR was less than two seconds for all the proposed cases here. We may confidently conclude that MO-GPR is a very suitable framework for online prognosis and practical implementation for lubricating oil degradation modeling, RUL prediction and predictive maintenance.

This work can be further extended to account for various other factors e.g. effect of imperfect maintenance, oil loss, operating conditions, environmental variations etc., which will form the scope of a future study that is currently in progress. It will also be beneficial to practically apply this framework to real condition monitored data sets from LCM and from several other industrial systems and applications to further confirm and validate the robustness of the MO-GPR model.

REFERENCES

[1] B. J. Roylance, "Ferrography—Then and now," *Tribology Int.*, vol. 38, no. 10, pp. 857–862, Oct. 2005.
[2] X. Yan, C. Sheng, J. Zhao, K. Yang, and Z. Li, "Study of on-line condition monitoring and fault feature extraction for marine diesel engines based on tribological information," *Proc. Inst. Mech. Eng., O, J. Risk Rel.*, vol. 229, no. 4, pp. 291–300, Aug. 2015.
[3] H. Powrie and A. Novis, "Gas path debris monitoring for F-35 joint strike fighter propulsion system PHM," in *Proc. IEEE Aerosp. Conf.*, Mar. 2006, p. 8.
[4] W. Cao, W. Chen, G. Dong, J. Wu, and Y. Xie, "Wear condition monitoring and working pattern recognition of piston rings and cylinder liners using on-line visual ferrograph," *Tribol. Trans.*, vol. 57, no. 4, pp. 690–699, Jul. 2014.
[5] X. Zhu, C. Zhong, and J. Zhe, "Lubricating oil conditioning sensors for online machine health monitoring—a review," *Tribol. Int.*, vol. 109, pp. 473–484, May 2017.
[6] L. Bo, X. Yinhu, F. Song, M. Junhong, and X. You-Bai, "A direct reflection OLVF debris detector based on dark-field imaging," *Meas. Sci. Technol.*, vol. 29, pp. 65–104, Apr. 2018.
[7] I. M. Flanagan, J. R. Jordan, and H. W. Whittington, "Wear-debris detection and analysis techniques for lubricant-based condition monitoring," *J. Phys. E, Sci. Instrum.*, vol. 21, no. 11, pp. 1011–1016, Nov. 1988.
[8] *A Standard Practice for Microscopic Characterization of Particles from In-Service Lubricants by Analytical Ferrograph*, Standard ASTM D7690-2011, ASTM International, West Conshohocken, PA, USA, 2011. [Online]. Available: www.astm.org
[9] W. Yuan, K. S. Chin, M. Hua, G. Dong, and C. Wang, "Shape classification of wear particles by image boundary analysis using machine learning algorithms," *Mech. Syst. Signal Process.*, vols. 72–73, pp. 346–358, May 2016.
[10] A. Becker, S. Abanteriba, S. Dutton, D. Forrester, and G. Rowlinson, "On the impact of fine filtration on spectrometric oil analysis and inductive wear debris sensors," *Proc. Inst. Mech. Eng. Part J, J. Eng. Tribol.*, vol. 230, no. 1, pp. 78–85, Jan. 2016.
[11] W. Cao, G. Dong, Y.-B. Xie, and Z. Peng, "Prediction of wear trend of engines via on-line wear debris monitoring," *Tribol. Int.*, vol. 120, pp. 510–519, Apr. 2018.
[12] B. Fan, B. Li, S. Feng, J. Mao, and Y.-B. Xie, "Modeling and experimental investigations on the relationship between wear debris concentration and wear rate in lubrication systems," *Tribol. Int.*, vol. 109, pp. 114–123, May 2017.
[13] J. F. S. Perez, J. A. Moreno, and F. Alhama, "Numerical simulation of high-temperature oxidation of lubricants using the network method numerical simulation of high-temperature oxidation of lubricants using the network method," *Chem. Eng. Commun.*, vol. 202, no. 7, pp. 982–991, 2015.
[14] A. K. S. Jardine, D. Lin, and D. Banjevic, "A review on machinery diagnostics and prognostics implementing condition-based maintenance," *Mech. Syst. Signal Process.*, vol. 20, no. 7, pp. 1483–1510, Oct. 2006.
[15] C. K. Tan, P. Irving, and D. Mba, "A comparative experimental study on the diagnostic and prognostic capabilities of acoustics emission, vibration and spectrometric oil analysis for spur gears," *Mech. Syst. Signal Process.*, vol. 21, no. 1, pp. 208–233, Jan. 2007.
[16] P. Thapliyal and G. D. Thakre, "Correlation study of physicochemical, rheological, and tribological parameters of engine oils," *Adv. Tribol.*, vol. 2017, Jun. 2017, Art. no. 1257607
[17] V. Dalis and L. Zak, "Approaches in correlation analysis and application on oil field data," *Appl. Mech. Mater.*, vol. 245, pp. 165–172, 2012.
[18] O. Alagoz, H. Hsu, A. J. Schaefer, and M. S. Roberts, "Markov decision processes: A tool for sequential decision making under uncertainty," *Med. Decis. Making*, vol. 30, no. 4, pp. 474–483, Jul. 2010.
[19] B. Ghodrati, "Reliability and operating environment based spare parts planning," Ph.D. dissertation, Dept. Division Operation Maintenance Eng., Luleå Univ. Technol., Luleå, Sweden, 2005.
[20] J. R. Ottewill and M. Orkisz, "Condition monitoring of gearboxes using synchronously averaged electric motor signals," *Mech. Syst. Signal Process.*, vol. 38, no. 2, pp. 482–498, Jul. 2013.

[21] S. Ebersbach, Z. Peng, and N. Kessissoglou, "Smart condition monitoring by integration of vibration oil and wear particle analysis," in *Proc. 14th Int. Congr. Sound Vibrat.*, Cairns, Australia, 2007, pp. 1–9.
[22] J. Wakiru, L. Pintelon, P. N. Muchiri, and P. Chemweno, "A statistical approach for analyzing used oil data and enhancing maintenance decision making: Case study of a thermal power," in *Proc. 2nd Int. Conf. Maintenance Eng. (IncoME-II)*, 2017, pp. 117–128.
[23] K. E. Spezzaferro, "Applying logistic regression to maintenance data to establish inspection intervals," in *Proc. Annu. Rel. Maintainability Symp.*, Jan. 1996, pp. 296–300.
[24] F. D. Samirmi, W. Tang, and H. Wu, "Feature selection in power transformer fault diagnosis based on dissolved gas analysis," in *Proc. IEEE PES ISGT Eur.*, Oct. 2013, pp. 1–5.
[25] J. Yan and J. Lee, "Degradation assessment and fault modes classification using logistic regression," *J. Manuf. Sci. Eng.*, vol. 127, no. 4, pp. 912–914, Nov. 2005.
[26] J. Phillips, E. Cripps, J. W. Lau, and M. R. Hodkiewicz, "Classifying machinery condition using oil samples and binary logistic regression," *Mech. Syst. Signal Process.*, vols. 60–61, pp. 316–325, Aug. 2015.
[27] D. Ide, A. Ruike, and M. Kimura, "Extraction of causalities and rules involved in wear of machinery from lubricating oil analysis data," in *Proc. 2nd Int. Conf. Inf. Process. Data Mining, Wireless Commun., Soc. Digit. Inf. Wireless Commun. (SDIWC)*, Wilmington, NC, USA, 2015, pp. 16–22.
[28] W. Caesarendra, A. Widodo, and B.-S. Yang, "Application of relevance vector machine and logistic regression for machine degradation assessment," *Mech. Syst. Signal Process.*, vol. 24, no. 4, pp. 1161–1171, May 2010.
[29] J. Wakiru, L. Pintelon, P. Chemweno, and P. N. Munchiri, "A decision tree-based classification framework for used oil analysis applying random forest feature selection," *J. Appl. Sci. Eng. Technol. Develop.*, vol. 3, pp. 90–100, 2018.
[30] Y. Du, T. Wu, and V. Makis, "Parameter estimation and remaining useful life prediction of lubricating oil with HMM," *Wear*, vols. 376–377, pp. 1227–1233, Apr. 2017.
[31] W. Wang, "Overview of a semi-stochastic filtering approach for residual life estimation with applications in condition based maintenance," *Proc. Inst. Mech. Eng. O, J. Risk Rel.*, vol. 225, no. 2, pp. 185–197, Jun. 2011.
[32] S. K. Yang, "A condition-based failure-prediction and processing-scheme for preventive maintenance," *IEEE Trans. Rel.*, vol. 52, no. 3, pp. 373–383, Sep. 2003.
[33] T. Wu, Y. Peng, H. Wu, X. Zhang, and J. Wang, "Full-life dynamic identification of wear state based on on-line wear debris image features," *Mech. Syst. Signal Process.*, vol. 42, nos. 1–2, pp. 404–414, Jan. 2014.
[34] M. Tanwar and N. Raghavan, "Lubricating oil degradation modeling and prognostics using the Wiener process," in *Proc. IEEE 3rd Int. Conf. Sens., Diagnostics, Prognostics, Control (SDPC)*, Beijing, China, Aug. 2019, pp. 1–5.
[35] M. Tanwar and N. Raghavan, "Lubrication oil degradation trajectory prognosis with ARIMA and Bayesian models," in *Proc. IEEE 3rd Int. Conf. Sens., Diagnostics, Prognostics, Control (SDPC)*, Beijing, China, Aug. 2019, pp. 1–6.
[36] R. R. Richardson, M. A. Osborne, and D. A. Howey, "Gaussian process regression for forecasting battery state of health," *J. Power Sources*, vol. 357, pp. 209–219, Jul. 2017.
[37] P. L. T. Duong, H. Park, and N. Raghavan, "Application of multi-output Gaussian process regression for remaining useful life prediction of light emitting diodes," *Microelectron. Rel.*, vols. 88–90, pp. 80–84, Sep. 2018.
[38] S. Hong, Z. Zhou, C. Lu, B. Wang, and T. Zhao, "Bearing remaining useful life prediction using Gaussian process regression with composite kernel functions," *J. Vibroeng.*, vol. 17, no. 2, pp. 695–704, 2015.
[39] Z. Chen, "Gaussian Process regression methods and extension for stock market prediction," Ph.D. dissertation, Dept. Math., Univ. Leicester, Leicester, U.K., 2017.
[40] V. N. A. Naikan and S. Kapur, "Reliability modelling and analysis of automobile engine oil," *Proc. Inst. Mech. Eng. D, J. Automobile Eng.*, vol. 220, no. 2, pp. 187–194, Feb. 2006.
[41] E. V. Bonilla, K. M. A. Chai, and C. K. I. Williams, "Multi-task Gaussian process prediction," *Proc. Adv. Neuaral Informat. Process. Syst.*, pp. 153–160, 2008.

MONIKA TANWAR received the B.E. degree in mechanical engineering from the University of Rajasthan, India, in 2006, the M.Tech. degree in industrial tribology and maintenance engineering from the Indian Institute of Technology (IIT) Delhi, India, in 2011, and the Ph.D. degree in maintenance engineering with the Department of Mechanical Engineering, IIT Delhi, in 2015. She was a Researcher with IFW, PZH, Leibniz University, Hannover. She is currently a Research Fellow with the Nano-Macro Reliability Lab, Singapore University of Technology and Design (SUTD) Singapore. Her research interests include predictive maintenance modeling, human error analysis, imperfect maintenance, maintenance performance, and reliability analysis.

NAGARAJAN RAGHAVAN (Member, IEEE) received the Ph.D. degree in microelectronics with the Division of Microelectronics, Nanyang Technological University (NTU), Singapore, in 2012. He was a Postdoctoral Fellow with the Massachusetts Institute of Technology (MIT), Boston, MA, USA, and with IMEC, Belgium, in joint association with the Katholieke Universiteit Leuven (KUL). He is currently an Assistant Professor with the Singapore University of Technology and Design (SUTD) in the Engineering Product Development (EPD) pillar. To date, he has authored or coauthored more than 185 international peer-reviewed publications and five invited book chapters as well. His works focus on reliability assessment, maintenance modeling, characterization, and lifetime prediction of nanoelectronic devices, as well as material design for reliability, uncertainty quantification and prognostics, and health management of electromechanical / industrial systems. He was an invited member of the IEEE GOLD committee, from 2012 to 2014. He was a recipient of the IEEE Electron Device Society (EDS) Early Career Award for 2016, Asia-Pacific recipient for the IEEE EDS Ph.D. Student Fellowship in 2011, and the IEEE Reliability Society Graduate Scholarship Award, in 2008. He serves as the General Chair for the IEEE IPFA 2020 at Singapore and has consistently served on the review committee for various IEEE Journals and conferences, including IRPS, IIRW, IPFA, and ESREF. He is also serving as an Associate Editor for IEEE Access.